Global dynamics of a Lotka–Volterra system in $\mathbb{R}^3$

Jaume Llibre, Y. Paulina Martínez, Claudia Valls

Global dynamics of a Lotka–Volterra system in $\mathbb{R}^3$

Jaume Llibre

Departament de Matemàtiques, Facultat de Ciències,
Universitat Autònoma de Barcelona, 08193 Bellaterra,
Barcelona, Catalonia, Spain
jllibre@mat.uab.cat

Y. Paulina Martínez

Centre de Recerca Matemática, 08193 Bellaterra,
Barcelona, Catalonia, Spain
yohanna.martinez@uab.cat

Claudia Valls

Center for Mathematical Analysis, Geometry and Dynamical Systems,
Departamento de Matemática, Instituto Superior Técnico,
Universidade de Lisboa, 1049-001 Lisboa, Portugal
cvalls@math.tecnico.ulisboa.pt

In this work we consider the Lotka–Volterra system in $\mathbb{R}^3$

$$\dot{x} = -x(x-y-z), \quad \dot{y} = -y(-x+y-z), \quad \dot{z} = -z(-x-y+z),$$

introduced recently in [7], and studied also in [8] and [14]. In the first two papers the authors mainly studied the integrability of this differential system, while in the third paper they studied the system as a Hamilton-Poisson system, and also started the analysis of its dynamics. Here we provide the global phase portraits of this 3-dimensional Lotka–Volterra system in the Poincaré ball, that is in $\mathbb{R}^3$ adding its extension to the infinity.

Keywords: Lotka–Volterra system; phase portraits; Poincaré ball.

2000 Mathematics Subject Classification: 37C10, 34C05.

1. Introduction and statement of the main results

The Lotka–Volterra systems, developed independently by Alfred J. Lotka in 1925 [9] and Vito Volterra in 1926 [15], were initially proposed as models for studying the interactions in two dimensions between species. Kolmogorov [5] in 1936 extended these systems to arbitrary dimension and degree, which are now called Kolmogorov systems.

The Lotka–Volterra systems have been applied to model different natural phenomena such as the time evolution of conflicting species in biology (which began with the work of May [10]), the evolution of competition between three species (studied by May and Leonard [11]), the evolution of electrons, ions and neutral species in plasma physics [6], chemical reactions [4], hydrodynamics [1], economics [13], etc.

In this work we consider the following Lotka–Volterra system

$$
\begin{aligned}
\dot{x} &= -x(x-y-z), \\
\dot{y} &= -y(-x+y-z), \\
\dot{z} &= -z(-x-y+z),
\end{aligned}
\tag{1.1}
$$

where the dot denotes derivative with respect to the time t.

The main goal of this work is to describe the global dynamics of the Lotka–Volterra system (1.1) in $\mathbb{R}^3$ adding the infinity, i.e. we are interested in describing the phase portraits of system (1.1) on the Poincaré ball $\mathbb{D}^3$. A first attempt to describe these phase portraits was done in [14] where the authors gave a Hamilton-Poisson formulation of system (1.1). Leach and Miritzis in [7] proved that system (1.1) has a first integral, and in [8] the authors proved that this system has the two independent first integrals $x(y-z)$ and $y(z-x)$. The existence of these first integrals has some consequences on the phase portrait of the system. Thus on the invariant plane $x = 0$ one gets that all trajectories are contained in the hyperbolas $yz = $ constant. On the other hand, a generic trajectory is contained in the elliptic curves intersection of the surfaces $x(y-z) = $ constant and $y(z-x) = $ constant. In any case these informations are not sufficient for obtaining the global phase portrait of system (1.1) in the Poincaré ball.

Our objective is to establish the α- and ω-limit of all the orbits of system (1.1) and to characterize the phase portrait of this system in the Poincaré ball $\mathbb{D}^3$. We recall that the Poincaré ball can be seen as the closed unit ball centered at the origin of $\mathbb{R}^3$, where its interior is identified with $\mathbb{R}^3$ and its boundary $\mathbb{S}^2$ is identified with the infinity of $\mathbb{R}^3$ (in the sense that in $\mathbb{R}^3$ we can go or come from infinity in as many directions as points has the 2-dimensional sphere $\mathbb{S}^2$).

A polynomial differential system in $\mathbb{R}^3$ (in the interior of $\mathbb{D}^3$) can be extended analytically to its boundary $\mathbb{S}^2$. This extension was done by the first time by Poincaré in [12] for polynomial differential systems in $\mathbb{R}^2$ and it is called the Poincaré compactification. In [2] the authors give an extension to polynomial differential systems in $\mathbb{R}^3$. For a brief introduction to Poincaré compactification see the appendix.

Two compactified polynomial differential systems in the Poincaré ball $\mathbb{D}^3$ are *topologically equivalent* if there is a homeomorphism of $\mathbb{D}^3$ which send orbits of one system into orbits of the other system, preserving or reversing the orientation of all orbits.

We note that system (1.1) has the symmetry $(x,y,z,t) \to (-x,-y-z,-t)$. Then it is sufficient to study its dynamics for $x \geq 0$.

In the next theorem we describe the phase portrait on the half-ball $x \geq 0$ of the Poincaré ball for the 3-dimensional Lotka–Volterra system (1.1).

Theorem 1.1. *The dynamics of the 3-dimensional Lotka–Volterra system* (1.1) *in the Poincaré ball is the following.*

(a) *The phase portraits on the invariant planes $x = 0$, $y = 0$ and $z = 0$ are shown in Figures* 1 *and* 2.

(b) *The phase portraits on the invariant planes $x = z$, $y = z$ and $x = y$ are shown in Figure* 3.

(c) *The phase portrait at infinity is topologically equivalent to the one of Figure* 4.

(d) *The phase portraits on the boundary of the twelve invariant regions obtained dividing the Poincaré ball by the six previous invariant planes in the region $x \geq 0$ are topologically equivalent to the ones shown in Figure* 6.

(e) *The phase portraits in the interior of the twelve invariant regions provided in statement* (d) *are topologically equivalent to the ones shown in Figure* 7. *Moreover the* α- *and* ω-*limits of each orbit in the interior of these regions are given in Table* 1.

The paper is organized as follows. In section 2 we study system (1.1) on the planes $x = 0$, $y = 0$, $z = 0$, $y = x$, $z = y$ and $z = x$, and we prove statements (a) and (b) of Theorem 1.1. In section 3 we study the infinite equilibria of system (1.1) and give the phase portraits on the Poincaré ball, proving statements (c), (d) and (e) of Theorem 1.1. In the appendix there is a brief description of the Poincaré compactification for polynomial differential systems in $\mathbb{R}^3$ and in $\mathbb{R}^2$.

2. Phase Portraits of system (1.1) on the planes

In this section we study all the phase portraits of the 3-dimensional Lotka–Volterra system (1.1) on the planes $x = 0$, $y = 0$, $z = 0$, $y = x$, $z = y$ and $z = x$.

First we point out that in [8] the authors proved that system (1.1) has the two independent first integrals

$$H_1 = (xyz)(x-y)(x-z)(y-z), \text{ and}$$
$$H_2 = x^2y^2 - x^2yz - xy^2z + x^2z^2 - xyz^2 + y^2z^2.$$

Moreover the unique irreducible Darboux polynomials with non-zero cofactor of system (1.1) are:

(1) x, y, z with cofactors $-(x-y-z)$, $-(-x+y+-z)$, and $-(-x+-y+z)$, respectively.
(2) $x-z$, $y-z$ and $z-x$ with cofactors $-(x-y+z)$, $-(-x+y+z)$, and $-(x+y-z)$, respectively.

We separate the study of the dynamics in the invariant planes in two cases.

2.1. *Phase portraits on the invariant planes* $x = 0$, $y = 0$ *and* $z = 0$

First note that system (1.1) on the planes $x = 0$, $y = 0$ and $z = 0$ are equivalent. In fact, system (1.1) on $x = 0$ is given by

$$\dot{y} = -y(y-z), \quad \dot{z} = -z(-y+z), \tag{2.1}$$

on $y = 0$ by

$$\dot{x} = -x(x-z), \quad \dot{z} = -z(-x+z), \tag{2.2}$$

and on $z = 0$ by

$$\dot{x} = -x(x-y), \quad \dot{y} = -y(-x+y). \tag{2.3}$$

Clearly system (2.1) and system (2.2) are equivalent through the change of variables $(y,z) \to (x,z)$, and system (2.3) is equivalent to the previous ones considering the changes of variables $(x,y) \to (x,z)$, or $(x,y) \to (y,z)$ to get system (2.2), or (2.1), respectively. Hence we are only going to analyze the global phase portraits of system (2.3).

We start with the study of the infinite singular points. For this purpose we use the Poincaré compactification of a polynomial differential systems in $\mathbb{R}^2$, see details in chapter 5 of [3]. System

(2.3) in the local chart U_1 is given by

$$\dot{z}_1 = -2z_1(-1+z_1), \quad \dot{z}_2 = -z_2(-1+z_1), \tag{2.4}$$

and in the local chart U_2 is

$$\dot{z}_1 = -2z_1(-1+z_1), \quad \dot{z}_2 = -z_2(-1+z_1). \tag{2.5}$$

From systems (2.4) and (2.5) we get that at infinity (i.e. at all points having the coordinate $z_2 = 0$) the origin of each chart is an equilibrium point. Moreover, in U_1 we have a second equilibrium point given by $(1,0)$. The eigenvalues of the linear part at the origins of U_1 and U_2 are 1 and 2, so they are unstable nodes. Note that since system (2.3) has degree 2 the corresponding equilibria on V_1 and V_2 will be stable nodes. The equilibrium $(1,0)$ in U_1 is not a hyperbolic equilibrium. It is at the infinity of the straight line $x = y$ which is filled of equilibria as will be seen later on in the next.

Now we study the finite singular points. System (2.3) has a straight line of equilibria given by $x = y$. Since $-x+y$ is a common factor of system (2.3), doing a reparametrization of the time, system (2.3) becomes

$$x' = x, \quad y' = -y. \tag{2.6}$$

It is known that the global dynamics of system (2.6) is the following: it has a saddle at the origin with stable separatrices on the y-axis and unstable separatrices on x-axis and at infinity it has infinite unstable nodes at the origins of U_1 and V_1 and infinite stable nodes at the origins of U_2 and V_2.

Going back through the reparametrization of time, taking into account the change of stability in the region $-x+y < 0$ and the straight line of finite equilibria on $-x+y = 0$, we can complete the global phase portrait of system (2.3) by using the Poincaré Bendixson Theorem (see [3]) connecting the separatrices of the saddle at the origin to the nodes at the infinity. Doing so we obtain the phase portrait described in Figure 1(a).
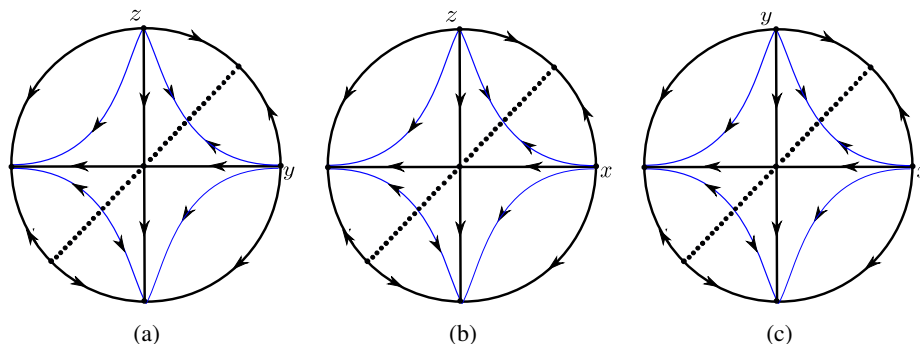

Fig. 1. Phase portraits of system (1.1) in the planes $x = 0$, $y = 0$ and $z = 0$, respectively.

The phase portraits in the planes $x = 0$, $y = 0$ and $z = 0$ in $\mathbb{R}^3$ are shown in Figure 2. This completes the proof of statement (a) of Theorem 1.1.
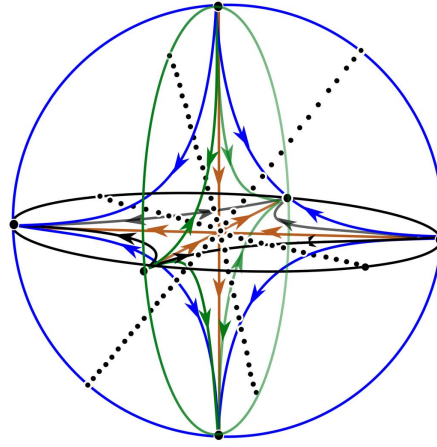
Fig. 2. Phase portrait of system (1.1) on the planes $x = 0$, $y = 0$, $z = 0$ inside the Poincaré ball.

2.2. *Phase portraits on the invariant planes $x = z$, $y = z$ and $y = x$*

Note that the dynamics of system (1.1) restricted to the plane $x = z$, to the plane $y = z$ and to the plane $y = x$ are topologically equivalent. Actually it is sufficient to study the phase portrait in the plane $x = z$ (taking $z \to x$) and inthis case system (1.1) takes the form

$$\dot{x} = xy, \quad \dot{y} = -y(y - 2x). \tag{2.7}$$

System (2.7) has the common factor y. Eliminating this common factor by reparametrizing the time, it becomes

$$x' = x, \quad y' = 2x - y, \tag{2.8}$$

whose phase portrait consists in a saddle at the origin with stable separatrices on the y axis and unstable separatrices on the straight line $x = y$.

At infinity we have that system (2.8) in the local chart U_1 is

$$z_1' = 2 - 2z_1, \quad z_2' = -z_2,$$

which has a unique equilibrium on $(1, 0)$ and it is a stable node. In the local chart V_1 it has another stable node. On the other hand, on the local chart U_2 system (2.8) writes as

$$z_1' = 2z_1(1 - z_1), \quad z_2' = (1 - 2z_1)z_2.$$

The origin is an equilibrium point which is an unstable node. The same stability has the origin of V_2. Observe that system (2.7) has the opposite stability in the region $y < 0$ than system (2.8).

From the previous analysis of system (2.8), considering the reparametrization done with the factor y, and due to the fact that there are not more finite equilibria, by the Poincaré Bendixson Theorem, we have that the separatrices of the saddle at the origin connect with the nodes at infinity. We can thus conclude that the phase portrait in the Poincaré disc of system (2.7) is the one described on Figure 3. Statement (b) of Theorem 1.1 has been proved.
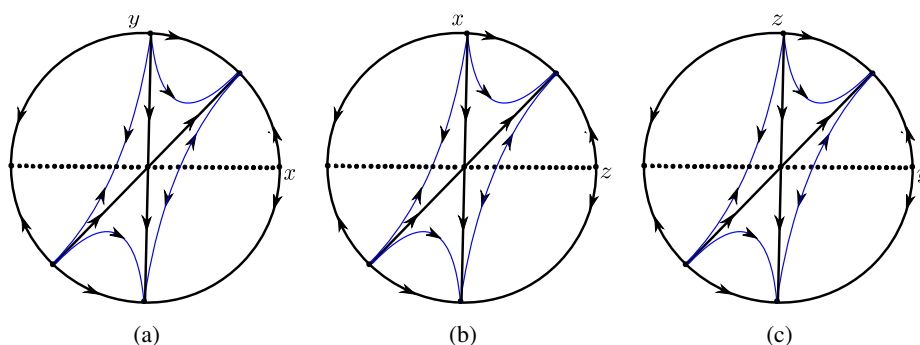
Fig. 3. Phase portraits of system (1.1) in the planes $z = x$, $y = z$ and $x = y$, respectively.

3. Dynamics on $\mathbb{R}^3$

In order to obtain the phase portrait in $\mathbb{R}^3$ of system (1.1) we first study the phase portrait at infinity using the Poincaré compactification (for details of the Poincaré compactification in $\mathbb{R}^3$, see appendix A.1).

System (1.1) in the local charts U_1, U_2 and U_3 are exactly the same, except for the meaning of the coordinates (z_1, z_2, z_3) (see (A.1), (A.2) and (A.3)). At infinity we have the following system in the local charts

$$z_1 = -2z_1(-1 + z_1), \quad z_2 = -2z_2(-1 + z_2), \quad z_3 = -z_3(-1 + z_1 + z_2). \tag{3.1}$$

Considering (3.1) on the local chart U_1, we have the four infinite equilibria (i.e, on $z_3 = 0$): the origin, $\hat{p}_1 = (0,0,0)$, $\hat{p}_2 = (1,0,0)$, $\hat{p}_3 = (0,1,0)$ and $\hat{p}_4 = (1,1,0)$. In the local chart U_2 the infinite equilibria on $z_1 = z_3 = 0$ are the origin of U_2, $\hat{p}_5 = (0,0,0)$ and $\hat{p}_6 = (0,1,0)$. Finally, in the local chart U_3 we have that the origin $\hat{p}_7 = (0,0,0)$ is an infinite equilibria.

All the infinite equilibria are at the infinity of the planes studied in section 2 and so their phase portraits are known. Due to the fact that the linear part of system (3.1) is

$$\begin{pmatrix} -2(z_1 - 1) - 2z_1 & 0 & 0 \\ 0 & -2(z_2 - 1) - 2z_2 & 0 \\ -z_3 & -z_3 & -z_1 - z_2 + 1 \end{pmatrix}$$

which is a diagonal matrix, it is easy to conclude that $\hat{p}_1$, $\hat{p}_5$ and $\hat{p}_7$ are unstable nodes, $\hat{p}_4$ is a stable node, that the eigenvalues of $\hat{p}_2$ are $-2, 2, 0$, and the eigenvalues of $\hat{p}_3$ and $\hat{p}_6$ are $2, -2, 0$. Thus, $\hat{p}_2, \hat{p}_3$ and $\hat{p}_6$ are saddles in the plane $z_3 = 0$.

In summary in the Poincaré ball we have 14 infinite equilibria. They are $p_1 = (1,0,0)$, $p_2 = (1,1,0)$, $p_3 = (1,0,1)$, $p_4 = (1,1,1)$, $p_5 = (0,1,0)$, $p_6 = (0,1,1)$ and $p_7 = (0,0,1)$ on the charts U_1, U_2 and U_3 and their corresponding antipodal equilibria on the local charts V_i (that we will denote by q_i the antipodal point of p_i) for $i = 1, 2, 3$.

Using the Poincaré-Bendixson Theorem we can characterize the connections between the separatrices of the saddles at p_2, p_3 and p_6 with the infinite nodes. Furthermore, these separatrices are on the invariant planes studied in section 2. The phase portrait at infinity is the one shown in Figure 4. This completes the proof of statement (c) of Theorem 1.1.
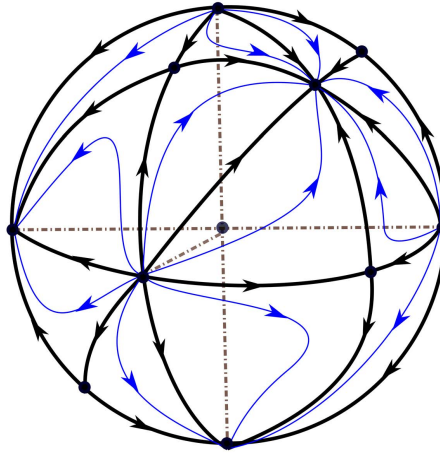
Fig. 4. Phase portrait of system (1.1) at infinity on the boundary of the Poincaré ball for $x \geq 0$.

On the other hand, the finite equilibria of system (1.1) are the origin and the straight lines of equilibria already mentioned in section 2. Then we can describe the phase portrait in the Poincaré ball.

In order to give an efficient description of the global dynamics of system (1.1) we separate the Poincaré ball in regions defined by the intersections of the planes $x = 0$, $y = 0$, $z = 0$, $x = y$, $x = z$ and $y = z$. There are 24 regions, all invariant by the flow of system (1.1). Due to the symmetry $(x, y, z, t) \to (-x, -y, -z, -t)$ it is sufficient to analyze the invariant regions contained in $x \geq 0$. These regions are

$$R_1 = \{(x, y, z) : 0 \leq y < x < z\}, \quad R_7 = \{(x, y, z) : y \leq 0 \leq x < z\},$$
$$R_2 = \{(x, y, z) : 0 \leq x < y < z\}, \quad R_8 = \{(x, y, z) : y \leq 0 \leq z < x\},$$
$$R_3 = \{(x, y, z) : 0 \leq x < z < y\}, \quad R_9 = \{(x, y, z) : z \leq 0 \leq y < x\},$$
$$R_4 = \{(x, y, z) : 0 \leq z < x < y\}, \quad R_{10} = \{(x, y, z) : z \leq 0 \leq x < y\},$$
$$R_5 = \{(x, y, z) : 0 \leq z < y < x\}, \quad R_{11} = \{(x, y, z) : z < y \leq 0 \leq x\},$$
$$R_6 = \{(x, y, z) : 0 \leq y < z < x\}, \quad R_{12} = \{(x, y, z) : y < z \leq 0 \leq x\}.$$

The mentioned regions R_1-R_{12} are shown in Figure 5. We note that the differential system is invariant under the cyclic permutation of the variables x, y, z, and consequently the dynamics on several of the regions R_k for $k = 1, \ldots, 12$ in which is divided the half-space $x \geq 0$ can be obtained one from the others. But in what follows we prefer to provide the dynamics in all these twelve regions because this facilitates understanding the motion between these regions.

To provide the phase portrait in each of these regions we describe first the phase portrait in the faces of each region, and after that the phase portrait in the interior of them. Note that in each region the isolated equilibria are on the vertices of the region and a segment filled of equilibria is on an edge of the region. We recall that one orbit in each face and one orbit in the interior are sufficient for determining the phase portraits in each invariant region. The edges of the regions are separatrices or segments filled of equilibria.

As an example we consider the region R_1. This region is a tetrahedron formed by three infinite equilibria p_3, p_4 and p_7 and the finite equilibrium at the origin θ. Note that it has one edge, given by $x = z$ and $y = 0$, which connects the vertex p_3 with θ filled of equilibria. The infinite equilibrium
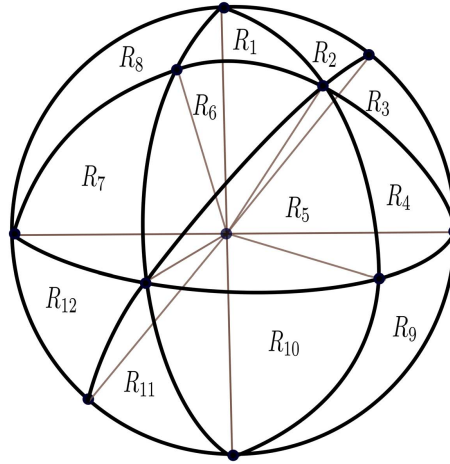
Fig. 5. Regions $R_1 - R_{12}$ on the Poincaré ball.

p_4 is an attractor and p_7 is a repeller. By the Poincaré-Bendixson Theorem we can establish the α- and ω-limits of all the orbits in this region.

In the faces of R_1 without a segment filled of equilibria all the orbits have their ω-limit in p_4 and their α-limit in p_7.

On the face formed by p_3, p_7 and θ the orbits have their α limit in p_7 and the ω-limit on the edge filled of equilibria.

On the face formed by p_3, p_4 and θ all orbits have their ω-limit at p_4 and their α-limit on the edge filled of equilibria.

Finally in the region R_1, by the Poincaré-Bendixson Theorem, we can conclude that an orbit in the interior of R_1 has its α-limit at p_7 and its ω-limit at p_4.

The phase portrait in the remaining regions can be characterized analogously. In Table 1 it is shown the α- and ω-limits for all orbits in the interior of each region.

	R_1, R_2	R_3, R_4	R_5, R_6	R_7, R_{12}	R_8	R_9	R_{10}, R_{11}
α-limit	p_7	p_5	p_1	p_1	p_7	p_5	p_1
ω-limit	p_4	p_4	p_4	q_5	q_5	q_7	q_7

Table 1. α- and ω-limits in the interior each invariant region R_1-R_{12}.

In Figure 6 it is shown the phase portraits on the boundary of the invariant regions, and one orbit in the interior of each invariant region is shown in Figure 7. These previous results prove statements (d) and (e) of Theorem 1.1 and complete the proof of Theorem 1.1.

A. Poincaré Compactification

We give a description of the Poincaré compactification in order to describe the phase portraits in the Poincaré ball. The Poincaré compactification of $\mathbb{R}^3$ is needed in the proof of Theorem 1.1.
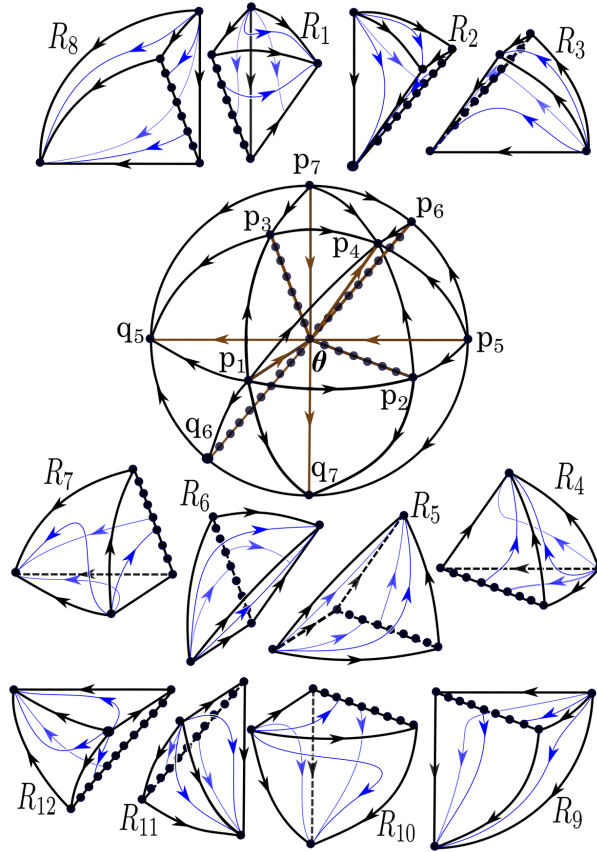
Fig. 6. Phase portraits of system (1.1) at the boundaries of the 12 regions contained in $x \geq 0$ obtained dividing the Poincaré ball by the six invariant planes, $x = 0$, $y = 0$, $z = 0$, $x = y$, $x = z$ and $y = z$.

We consider a polynomial vector field $\mathscr{X} = (P, Q, R)$ associated to the polynomial differential system

$$\dot{x}_1 = P(x_1, x_2, x_3), \qquad \dot{x}_2 = Q(x_1, x_2, x_3), \qquad \dot{x}_3 = R(x_1, x_2, x_3).$$

The degree n of $\mathscr{X}$ is defined as $n = \max\{\deg(P), \deg(Q), \deg(R)\}$.

Now we shall describe the equations of the Poincaré compactification of a polynomial differential system in $\mathbb{R}^3$.

We consider the local charts (U_k, ϕ_k) and (V_k, ψ_k) for $k = 1, 2$ on the disc $\mathbb{D}^3$ defined by

$$U_k = \{x = (x_1, x_2, x_3) \in \mathbb{D}^3 : x_k > 0\},$$
$$V_k = \{x = (x_1, x_2, x_3) \in \mathbb{D}^3 : x_k < 0\},$$

where the diffeomorphisms $\phi_k : U_k \to \mathbb{R}^3$ for $k = 1, 2, 3$ are

$$\phi_1(x) = \left(\frac{x_2}{x_1}, \frac{x_3}{x_1}, \frac{1}{x_1}\right) = (z_1, z_2, z_3), \quad \phi_2(x) = \left(\frac{x_1}{x_2}, \frac{x_3}{x_2}, \frac{1}{x_2}\right) = (z_1, z_2, z_3),$$

$$\phi_3(x) = \left(\frac{x_1}{x_3}, \frac{x_2}{x_3}, \frac{1}{x_3}\right) = (z_1, z_2, z_3),$$
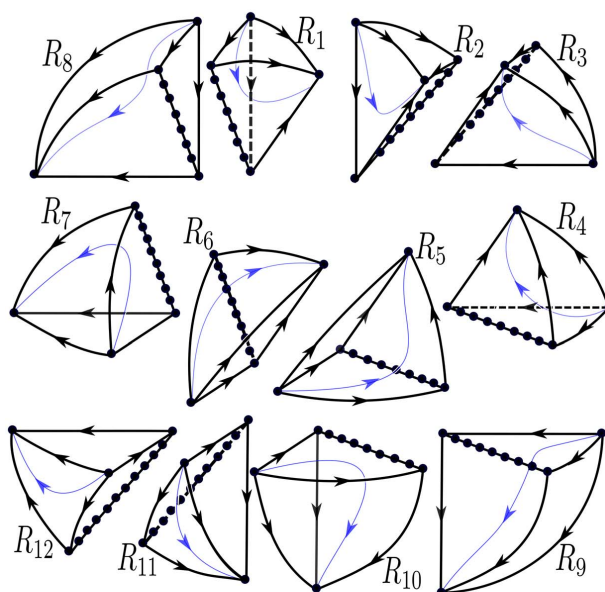
and $\psi_k(x) = -\phi_k(x)$.

Fig. 7. Phase portraits of system (1.1) in the interior of the invariant regions.

Note that the coordinates (z_1, z_2, z_3) have different meaning depending on local chart, but the points at infinity, i.e. the points of the boundary $\mathbb{S}^2$ of $\mathbb{D}^3$ have all the coordinate $z_3 = 0$.

Now we give the expression of the compactified vector field $p(\mathscr{X})$ of the polynomial vector field $X = (P, Q, R)$ in each local chart. The expression of the compactified analytical vector field $p(\mathscr{X})$ of $\mathscr{X}$ of degree n on the local chart U_1 of $\mathbb{D}^3$ is

$$z_3^n \left(-z_1 P(z) + Q(z), -z_2 P(z) + R(z), -z_3 P(z) \right), \tag{A.1}$$

where $z = (1/z_3, z_1/z_3, z_2/z_3)$.

In a similar way the expression of $p(\mathscr{X})$ in U_2 is

$$z_3^n \left(-z_1 Q(z) + P(z), -z_2 Q(z) + R(z), -z_2 Q(z) \right), \tag{A.2}$$

where $z = (z_1/z_3, 1/z_3, z_2/z_3)$.

Finally the vector field $p(\mathscr{X})$ in U_3 is

$$z_3^n \left(-z_1 R(z) + P(z), -z_2 R(z) + Q(z), -z_2 R(z) \right), \tag{A.3}$$

where $z = (z_1/z_3, z_2/z_3, 1/z_3)$.

The singular points of $p(\mathscr{X})$ which are on the boundary $\mathbb{S}^2$ of $\mathbb{D}^3$ (at $z_3 = 0$) are called *infinite singular points*, and we call *finite singular points* the ones which are in the interior of $\mathbb{D}^3$.

From equations (A.1), (A.2) and (A.3) it follows that the infinity $\mathbb{S}^2$ of the Poincaré ball is invariant under the flow of the compactified vector field $p(\mathscr{X})$. For studying its infinite singular points we only need to study the ones that are on the local chart U_1, in U_2 with $z_1 = 0$, and the origin of the local chart U_3 in case that this is a singular point.

The expression for $p(\mathscr{X})$ in the local chart V_k is the same as in U_k multiplied by $(-1)^{n-1}$. Therefore the infinite singular points appear on pairs diametrally opposite on $\mathbb{S}^2$ with the same

stability if *n* is odd and with the opposite stability if *n* is even. For more details on the Poincaré compactification in $\mathbb{R}^3$ see [2].

As we said in the introduction two compactified polynomial differential systems in the Poincaré ball $\mathbb{D}^3$ are *topologically equivalent* if there is a homeomorphism of $\mathbb{D}^3$ sending orbits of one system to orbits of the other system, either preserving or reversing the orientation of the orbits.

Acknowledgements

References

[1] F.H. Busse, *Transition to turbulence via the statistical limit cycle route*, In H. Haken, editor, Chaos and Order in Nature, Berlin, Heidelberg (Springer, 1981), 36–44.

[2] A. Cima and J. Llibre, Bounded polynomial vector fields, *Trans. Amer. Math. Soc.*, **318** (2) (1990), 577–579.

[3] F. Dumortier, J. Llibre, and J.C. Artés, *Qualitative theory of planar differential systems*, Universitext, Berlin (Springer, 2006).

[4] R. Hering, Oscillations in Lotka–Volterra systems of chemical reactions, *J. Math. Chem.*, **5** (1990), 197–202.

[5] A. Kolmogorov, Sulla teoria di volterra della lotta per l'esistenza, *Giornale dell' Istituto Italiano degli Attuari*, **7** (1936), 74–80.

[6] G. Laval and R. Pellat, Plasma physics (Les Houches), *Proc. Summer School of Theoretical Physics*, (1975), 261.

[7] P. Leach and J. Miritzis, Competing species: Integrability and stability, *J. Nonlinear Math. Phys.*, **11** (2006), 123–133.

[8] J. Llibre and C. Valls, Polynomial, rational and analytic first integrals for a family of 3-dimensional Lotka-Volterra systems, *Zeitschrift für angewandte Mathematik und Physik*, **62** (5) (2011), 761–777.

[9] A.J. Lotka, *Elements of physical biology*, Science Progress in the Twentieth Century (1919-1933), **21** (82) (1926), 341–343.

[10] R.M. May, *Stability and complexity in model ecosystems*, Princeton University Press Princeton, N.J. (1973).

[11] R.M. May and W. Leonard, Nonlinear aspects of competition between three species, *SIAM J. Appl. Math.*, **29** (1975), 243–253.

[12] H. Poincaré, Sur les courbes définies par une équation différentielle, Œuvres Complètes, **1** Theorem XVII (1928).

[13] S. Solomon and P. Richmond, Stable power laws in variable economies, Lotka–Volterra implies pareto-zipf, *The European Physical Journal B - Condensed Matter and Complex Systems*, **27** (2) (2002), 257–261.

[14] R.M. Tudoran and A. Girban, On a hamiltonian version of a three-dimensional Lotka–Volterra system, *Nonlinear Analysis-Real World Application*, **13** (2012), 2304–2312.

[15] V. Volterra, Variazioni e uttuazioni del numero d'individui in specie animali conviventi, *Memoire della R. Accademia Nazionale dei Lincei*, **CCCCXXIII** (II) (1926), 558–560.